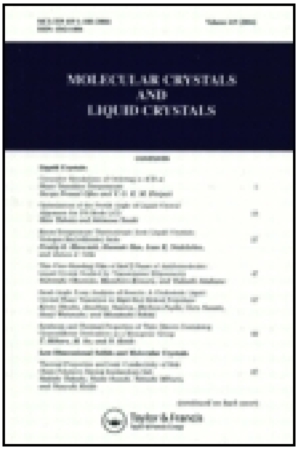

Molecular Crystals and Liquid Crystals
Publication details, including instructions for authors and subscription information:
http://www.tandfonline.com/loi/gmcl16

Structure of Doped Polymers

V. Enkelmann [a] , G. Lieser [a] , M. Monkenbusch [a] , W. Müller [a] & G. Wegner [a]

[a] Intitut für Makromolekulare, Chemie Stefan-Meier-Str. 31, D-7800, Freiburg, Germany

Version of record first published: 19 Dec 2006.

To cite this article: V. Enkelmann , G. Lieser , M. Monkenbusch , W. Müller & G. Wegner (1981): Structure of Doped Polymers, Molecular Crystals and Liquid Crystals, 77:1-4, 111-123

To link to this article: http://dx.doi.org/10.1080/00268948108075233

Mol. Cryst. Liq. Cryst., 1981, Vol. 77, pp. 111-123
0026-8941/81/7701-0111$06.50/0

Printed in the United States of America

(Proceedings of the International Conference on Low-Dimensional Conductors, Boulder, Colorado, August 1981)

STRUCTURE OF DOPED POLYMERS

V. ENKELMANN, G. LIESER, M. MONKENBUSCH,
W. MÜLLER and G. WEGNER
Institut für Makromolekulare Chemie
Stefan-Meier-Str. 31
D-7800 Freiburg, Germany

Received for publication August 17, 1981

Studies of the synthesis, molecular weight, structure and morphology of polyacetylene (PA) indicate that the average length of linear chain segments between structural defects like crosslinks and chain folds is of the order of 20 units. Several models for the crystal structure of trans PA are given. The influence of the morphology on the mechanism of charge transport is discussed. The doping is found to be inhomogeneous and the macroscopic conductivity is controlled by the topology of interlamellar contacts.

Relative to other molecular metals polyacetylene (PA) appears to be poorly characterized with respect to crystal structure and polymer morphology. This comes mainly from the fact that PA prepared by the more usual methods is insoluble so that the morphology and structure are determined by the reaction conditions and cannot be changed subsequently[1]. In addition, it should be pointed out that the polymerization itself is no equilibrium process but can be described as a simultaneous polymerization and crystallization leading to a highly complex and defect-rich structure. The conjugation length is limited by two kinds of defects, crosslinks (chemical defects) and chain folds (physical defects) so that the average length of linear chain segments is of the order of 20 units[2-5].

The kinetics of the crosslinking reaction depend on the polymerization conditions like catalyst, temperature and solvent. Under carefully optimized conditions using the Luttinger catalyst ($Co(NO_3)_2$/$NaBH_4$)[6] at low temperatureslinear PA can be obtained which can be quantitatively chlorinated under mild conditions (-30°C) to give a completely soluble derivative. It should be pointed out that the chlorination should be carried out immediately after the polymerization. If kept for some time even at low temperatures the crosslinking reaction proceeds and an insoluble fraction is observed.

In Fig. 1 gel permeation chromatograms for three representative samples are shown together with the dependence of the insoluble fraction on storage time at 243 K. It can be seen that the molecular weight distribution broadens and the average molecular weight is shifted to higher values. In combination with the observation of the insoluble fraction this clearly indicates the existence of crosslinks in PA and should be taken into consideration when discussing doping and conductivity.

It is interesting to note that PA prepared according to Shirakawa[1] can be chlorinated as well but even if the reaction is carried out immediately following the polymerization the derivatives are not completely soluble but resemble both in their insoluble fraction and molecular weight distribution the Luttinger PA stored for 16 hours at 243 K (Fig. 1).

MORPHOLOGY OF POLYACETYLENE

Independently of the polymerization method and the catalyst type used the same overall morphology is obtained. A typical transmission electron micrograph of Shirakawa PA is shown in Fig. 2. The morphology is characterized by a pseudofibrillar arrangements of aggregations of small irregular shaped lamellar particles with typically a few hundred Å diameter and a thickness of 50 to 100 Å forming a loose network. It should be emphasized at this point that the strings of polymer material shown in Fig. 2 cannot be interpreted as fibrils since no preferential orientation of the polymer chains along these morphological features is observed.

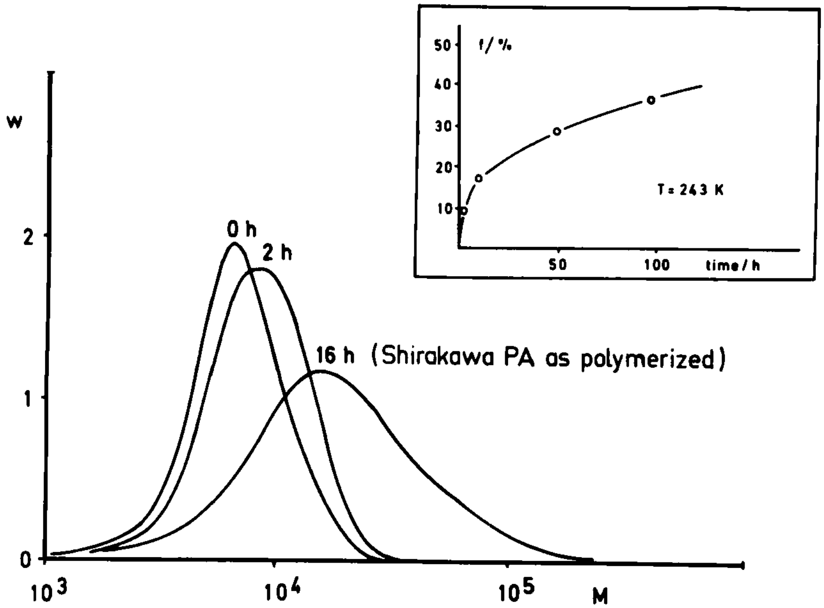

FIGURE 1 GPC diagrams for chlorinated PA after different storage times after polymerization at 243 K. The insert shows the increase of the insoluble fraction after chlorination.

Electron diffraction patterns obtained from selected areas from these strings show only Debye rings which can be interpreted as scattering of uniaxial oriented powders with the chain axis parallel to the primary beam since only hk0 reflections are observed. Comparison of the particle thickness and the determined average molecular weights indicate the existence of chain folds in PA. A detailed description of experimental techniques and the interpretation of the morphological and scattering data is given elsewhere[4,5,7]. The morphological model of PA which has been drived from these studies is schematically shown in Fig. 3

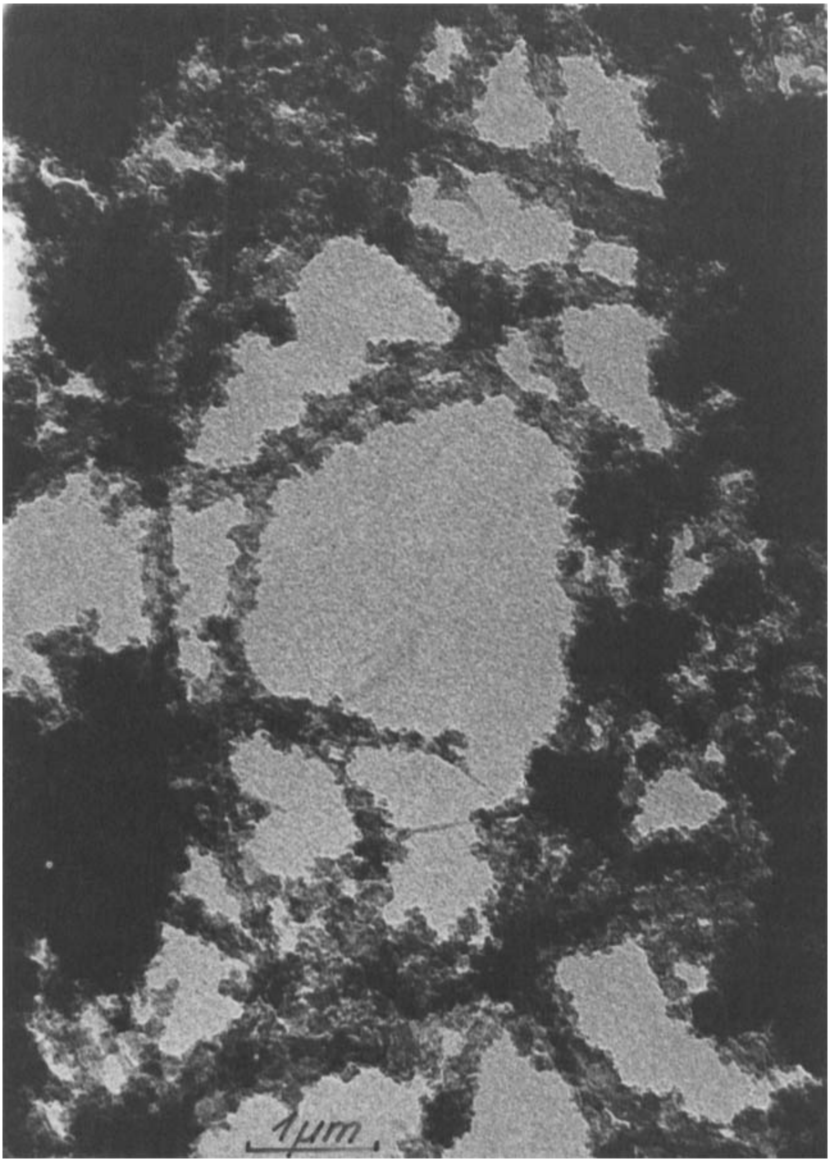

FIGURE 2 Transmission electron micrograph of Shirakawa polyacetylene.

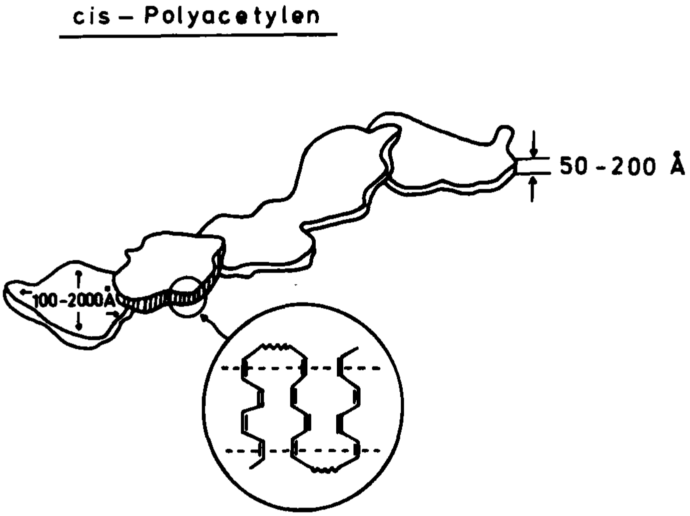

FIGURE 3 Model for the morphology of PA.

CRYSTAL STRUCTURE OF TRANS POLYACETYLENE

Another point of particular interest is the crystal structure of PA. Several models have been proposed both for the cis and trans isomers[3,4,8,9]. Unfortunately the X-ray diffraction data on PA provide only very limited information so that a structure analysis on this basis would fail. In this situation it seemed desirable to do packing calculations in order to analyze which structures are favored with respect to lattice energy and to compare these with the packing found in various oligoene model compounds $R_1-(CH=CH)_n-R_2$ and to the structural models for PA. This is of special importance since the polymerization and isomerization are no equilibrium processes and it can be imagined that several different packing arrangements could result from differences in the sample history. The results of our packing calculations the details of which will be published elsewhere[10] are shown in Fig. 4 and Fig. 5 and are summarized in Table 1,2,3 and 4.

The minimum packing energy configurations listed can be divided into oblique and rectangular cells. However, it should be emphasized at this

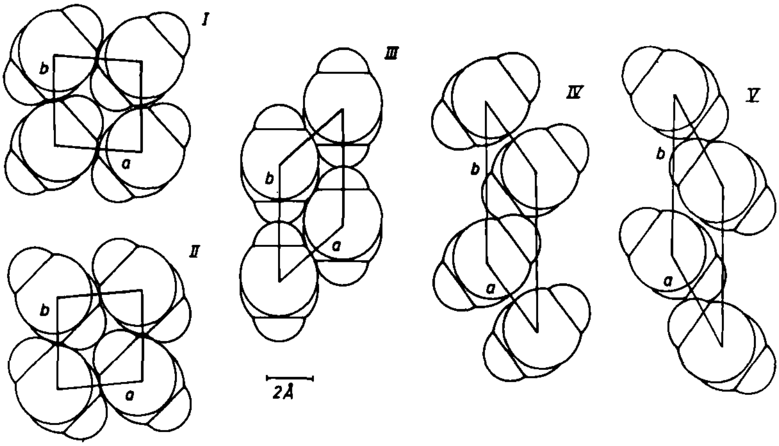

Figure 4 Minimum packing energy configurations for trans PA chains.

Table 1 Minimum packing energy configurations[a]

	I	II	III	IV	V	VI
a/Å	3.76	3.72	3.66	3.59	4.31	6.84
b/Å	3.77	3.82	4.85	6.65	6.63	3.94
γ/°	95	85	49	144	150	90
ϕ/°	48	129	41	90	25	56
F/eV	-0.402	-0.400	-0.390	-0.397	-0.392	-0.826
D_x/gcm^{-3}	1.25	1.25	1.25	1.27	1.26	1.24

[a] F is the packing energy and ϕ the setting angle

Table 2 Minimum packing energy configurations

	VII	VIII	IX	X	XI	XIV
a/Å	5.55	6.94	5.75	4.62	4.51	3.97
b/Å	4.86	3.80	4.80	6.99	7.16	7.01
β/°	90	90	90	124	123	92
ϕ/°	90	50	85	130	44	126
F/ev	-0.798	-0.863	-0.774	-0.876	-0.863	-0.822
D_x/gcm^{-3}	1.23	1.26	1.21	1.30	1.29	1.27

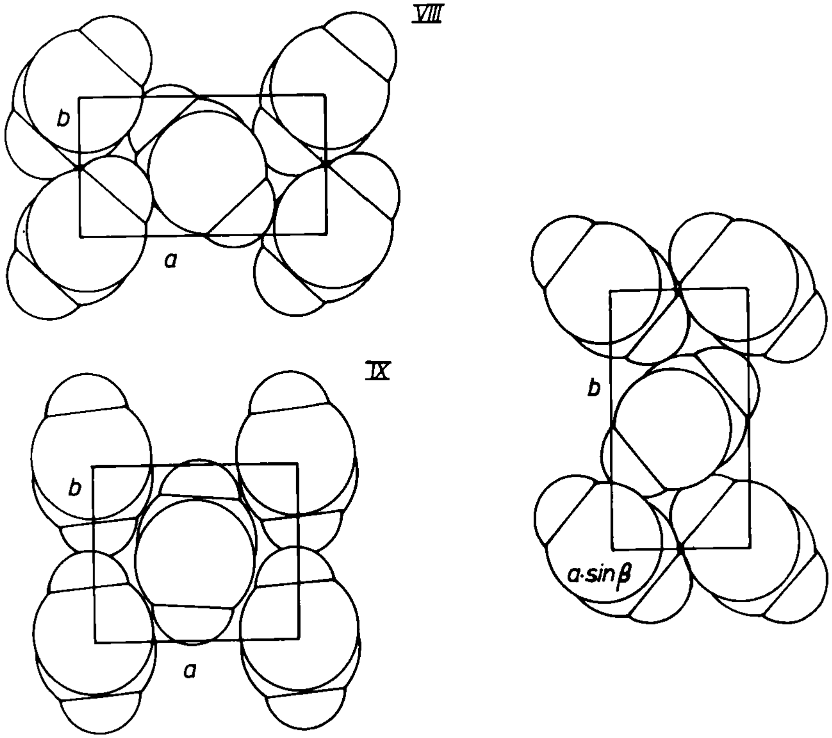

FIGURE 5 Minimum packing energy configurations for trans PA chains

Table 3 Packing of polyacetylene chains in model compounds $R_1-(CH=CH)_n-R_2$

R_1	-COOH	-CN	-Ph	-Ph
R_2	$-CH_3$	-CN	-Ph	-Ph
n	3	4	3,4,5	3,4,5
$\beta/^\circ$	90	90	99	124
$\gamma/^\circ$	99	147	90	90
a/Å	4.03	3.98	4.24	5.07
b/Å	4.07	6.34	7.60	7.45
c/Å	2.44	2.44	2.45	2.48
$\phi/^\circ$	50	43	140	150
D_x/gcm^{-3}	1.09	1.29	1.12	1.13

Table 4 Structural models for trans PA

a/Å	3.73(5)	5.62(5)	7.32
b/Å	3.73(5)	4.92(2)	4.24
c/Å	2.44(2)	2.592(5)	2.44
$\gamma/^{\circ}$	98(2)	90	90
$\phi/^{\circ}$	--	--	24
D_x/gcm^{-3}	1.27	1.20	1.13
ref.	4	4	8

point that trans PA with a bond alternation cannot crystallize in orthorhombic structures since the symmetry of orthorhombic space groups requires equal bond lengths.

Inspection of the Tables 1 and 2 shows that all calculated structures have virtually identical packing energies. The calculated densities of the

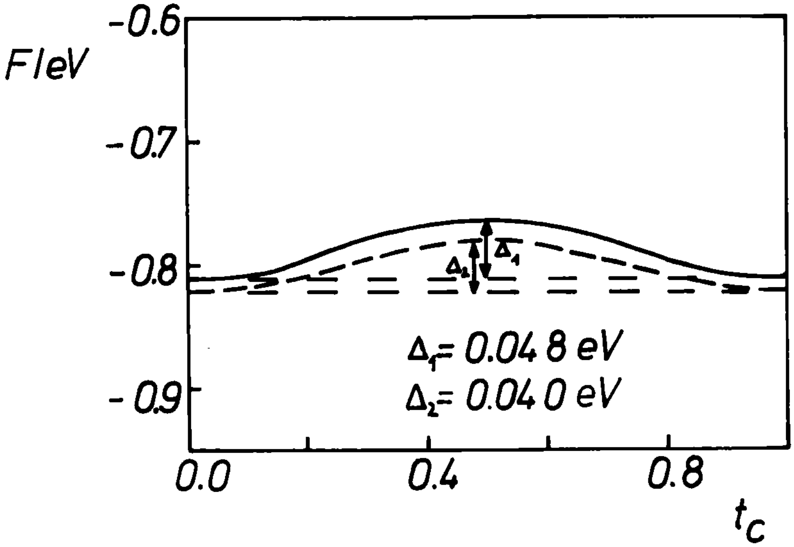

FIGURE 6 Dependence of the packing energy F on the translation of the second chain t_c along c in structure VIII (solid line) and in structure X (broken line)

oligoene model compounds are smaller due to end-group packing effects. Another interesting feature of the packing calculations is the fact that they reveal that the packing energy is nearly independent of translations of neighboring chains in the c direction (Fig. 6). This suggests that also nematic structures are highly probable.

MORPHOLOGY AND PROPERTIES

The highly complex lamellar morphology of PA prepared by the usual methods[1,12] with linear chain segments of limited length should be taken into consideration in the attempts to theoretically describe the conductivity of doped polymers. There must be a finite probability for an interchain charge transfer in order to allow charge transport over chain folds and crosslinks. The nature of such charge transfer interactions of simple

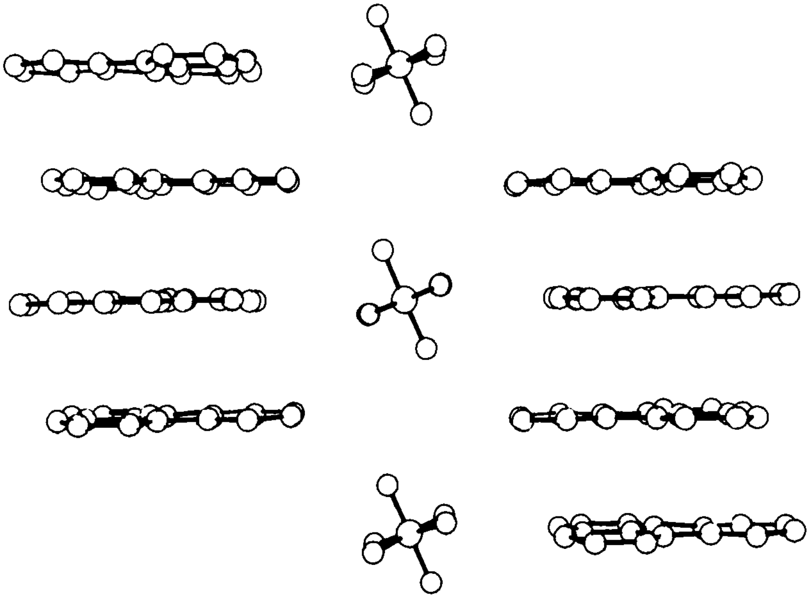

FIGURE 7 Crystal structure of the model complex Fluoranthene$_2$PF$_6$

hydrocarbons can be studied in the highly conductive radical cation salts which have been recently synthesized by anodic oxidation of simple arenes[13-16]. A representative crystal structure for this new family of organic metals is shown in Fig. 7. We tend to assume that the same charge transfer interaction is found in doped PA and other conducting polymers. This is schematically represented in Fig. 8. The radical cations are formed by attack of the dopant which is possible from both sides of the lamellae. In a first stage the dopant is absorbed at the surface and could eventually intercalate the structure. By formation of complexes of the same kind as found in the radical cation salts the created charge is delocalized both in the chain direction between chain folds and perpendicular to it. The following chemical equilibria are possible in this model:

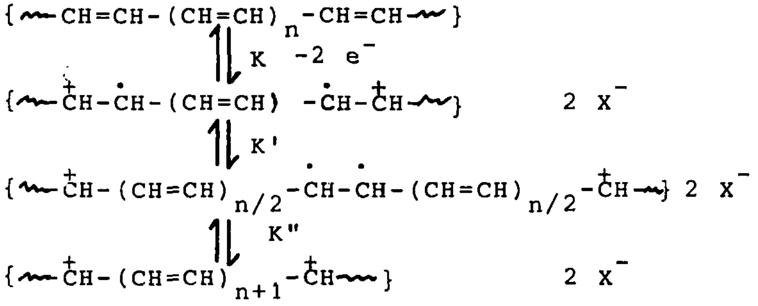

$$\{\sim CH{=}CH-(CH{=}CH)_n-CH{=}CH\sim\}$$
$$\Big\updownarrow K \quad -2\,e^-$$
$$\{\sim\overset{+}{C}H-\overset{\bullet}{C}H-(CH{=}CH)\ -\overset{\bullet}{C}H-\overset{+}{C}H\sim\} \qquad 2\ X^-$$
$$\Big\updownarrow K'$$
$$\{\sim\overset{+}{C}H-(CH{=}CH)_{n/2}-\overset{\bullet}{C}H-\overset{\bullet}{C}H-(CH{=}CH)_{n/2}-\overset{+}{C}H\sim\}\ 2\ X^-$$
$$\Big\updownarrow K''$$
$$\{\sim\overset{+}{C}H-(CH{=}CH)_{n+1}-\overset{+}{C}H\sim\} \qquad 2\ X^-$$

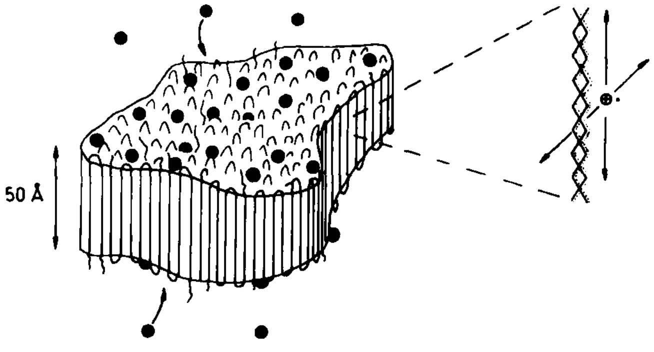

FIGURE 8 Model for the doped lamellae

This model only describes charge transfer within the morphological unit. It is clear that in this morphology interlamellar contacts play an important role for the macroscopic conductivity which is probably not an intrinsic property of the doped polymer itself but is a function of the particle network. Indeed we have observed that the setting process in which the individual particles prepared in the Luttinger process aggregated to free standing PA films of considerable strength and conductivities (SbF_5 or electrochemically doped) of several hundred Ω^{-1} cm^{-1} is very important and must be carefully controlled in order to obtain good quality samples.

In our experience the doping process is inhomogeneous. A partially doped sample will show

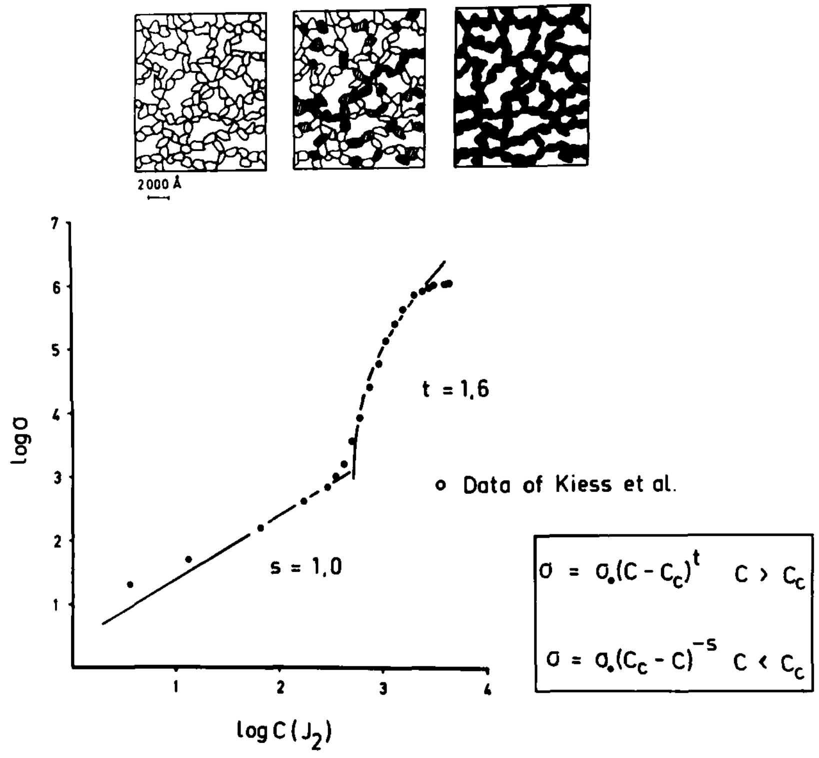

FIGURE 9 Dependence of the specific conductivity of I_2 doped PA on the iodine concentration. Data points from Kiess *et al.*[18]. Solid line: Percolation theory applied with equations and exponents given

in the electron microscope highly doped and totally unreacted regions. This observation leads to the assumption that the macroscopic conductivity of PA depends strongly on the sample and could be treated by statistical methods like the percolation theory[17]. This is shown in Fig. 9 for iodine doped PA[18]. The inserts in this Figure schematically represent the structure of the inhomogeneously doped polymer below at and above the critical concentration. The critical exponents s and t used for the fit are those predicted for a random three dimensional network.

REFERENCES

1. H. Shirakawa and S. Ikeda, Polymer J. 2, 231 (1971).
2. V. Enkelmann, W. Müller and G. Wegner, Synth. Metals 1, 185 (1980).
3. G. Lieser, G. Wegner, W. Müller and V. Enkelmann, Makromol. Chem. Rapid Comm. 1, 621 (1980).
4. G. Lieser, G. Wegner, W. Müller, V. Enkelmann and W.H. Meyer, Makromol. Chem. Rapid Comm. 1, 627 (1980).
5. H. Kuzmany, Phys. Stat. Sol. (b) 97, 521 (1980).
6. L.B. Luttinger, J. Org. Chem. 27, 1591 (1962).
7. G. Lieser, M. Monkenbusch, V. Enkelmann and G. Wegner, Mol. Cryst. Liq. Cryst., in preparation.
8. K. Shimamura, F.E. Karasz, J.A. Hirsch and J.C.W. Chien, Makromol. Chem., in press.
9. R.H. Baughman, S.L. Hsu, G.P. Pez and A.J. Signorelli, J. Chem. Phys. 68, 5405 (1978).
10. V. Enkelmann, M. Monkenbusch and G. Wegner, Polymer, submitted.
11. W. Drenth and E.H. Wibenga, Rec. trav. chim. 73, 218 (1954); Acta Cryst. 8, 755 (1955).
12. A.G. MacDiarmid and A.J. Heeger in Molecular Metals, ed. W.E. Hatfield (Plenum Press, New York and London, 1979).
13. H.P. Fritz, H. Gebauer, P. Friedrich, P. Ecker, R. Artes and U. Schubert, Z. Naturforsch. (b) 33, 498 (1978).
14. G. Wegner, C. Kröhnke and V. Enkelmann, Angew. Chem. 92, 941 (1980).
15. H.J. Keller, D. Nöthe, H. Pritzkow, D. Wehe, M. Werner, P. Koch and D. Schweizer, Mol. Cryst.

Liq. Cryst. 62, 181 (1981).
16. V. Enkelmann, B.S. Morra, C. Kröhnke, G. Wegner and J. Heinze, Chem. Phys., in press.
17. S. Kirkpatrick, Rev. Mod. Phys. 45, 574 (1973).
18. H. Kiess, W.H. Meyer, D. Baeriswyl and G. Harbecke, J. Electron. Mater. 9, 763 (1980).